Development 128, 5039-5050 (2001)
Printed in Great Britain © The Company of Biologists Limited 2001
DEV3523

unc-83 encodes a novel component of the nuclear envelope and is essential for proper nuclear migration

Daniel A. Starr[1], Greg J. Hermann[2], Christian J. Malone[1,*], William Fixsen[3,†], James R. Priess[2], H. Robert Horvitz[3] and Min Han[1,‡]

[1]Howard Hughes Medical Institute and Department of Molecular, Cellular and Developmental Biology, University of Colorado, Boulder, CO 80309, USA
[2]Howard Hughes Medical Institute and Division of Basic Sciences, Fred Hutchinson Cancer Research Center, Seattle, WA 98109, USA
[3]Howard Hughes Medical Institute and Department of Biology, Massachusetts Institute of Technology, Cambridge, MA 02139, USA
*Present address: Laboratory of Molecular Biology, University of Wisconsin, Madison, WI 53706, USA
†Present address: Department of Continuing Education, Harvard University, Cambridge, MA 02138, USA
‡Author for correspondence (e-mail: mhan@colorado.edu)

Accepted 20 September 2001

SUMMARY

Nuclear migration plays an essential role in the growth and development of a wide variety of eukaryotes. Mutations in *unc-84*, which encodes a conserved component of the nuclear envelope, have been shown to disrupt nuclear migration in two *C. elegans* tissues. We show that mutations in *unc-83* disrupt nuclear migration in a similar manner in migrating P cells, hyp7 precursors and the intestinal primordium, but have no obvious defects in the association of centrosomes with nuclei or the structure of the nuclear lamina of migrating nuclei. We also show that *unc-83* encodes a novel transmembrane protein. We identified three *unc-83* transcripts that are expressed in a tissue-specific manner. Antibodies against UNC-83 co-localized to the nuclear envelope with lamin and UNC-84. Unlike UNC-84, UNC-83 localized to only specific nuclei, many of which were migratory. UNC-83 failed to localize to the nuclear envelope in *unc-84* mutants with lesions in the conserved SUN domain of UNC-84, and UNC-83 interacted with the SUN domain of UNC-84 in vitro, suggesting that these two proteins function together during nuclear migration. We favor a model in which UNC-84 directly recruits UNC-83 to the nuclear envelope where they help transfer force between the cytoskeleton and the nucleus.

Key words: UNC-83, UNC-84, Nuclear envelope, Nuclear migration, *C. elegans*

INTRODUCTION

Many cells have mechanisms to control the position of the nucleus during development and growth. For example, nuclei may migrate before an asymmetric cell division, and several epithelial organs show highly polarized nuclear positioning (Leung et al., 1999; Tomlinson, 1985). Defects in nuclear migration may lead to human disease. Mutations in *LIS1* cause type I lissencephaly, in which neural migration into the cortex is disrupted (Dobyns and Truwit, 1995; Reiner et al., 1993). *LIS1* is the human homolog of *Aspergillus NudF*. Mutations in *NudF* disrupt nuclear positioning in filamentous fungi, suggesting that mutations in *LIS1* may cause lissencephaly by blocking nuclear migration (Morris, 2000). In most cases studied, nuclear migration appears to involve the centrosome and various motor proteins associated with the microtubule cytoskeleton (Raff and Glover, 1989). The centrosome is closely associated with the nucleus and may provide the force that drives the nucleus to a particular place in the cell (Reinsch and Gonczy, 1998). Microtubules, in coordination with molecular motors and associated machinery, play essential roles in various nuclear migration events (Morris, 2000; Reinsch and Gonczy, 1998). In budding yeast, dynein, dynactin and kinesins function to position the nucleus in preparation for cell division (Morris, 2000). Nuclear migration in the *Drosophila* eye involves the Glued protein, a component of dynactin, and the Klarischst protein, which plays a role regulating microtubules during nuclear migration (Fan and Ready, 1997; Mosley-Bishop et al., 1999). Not all nuclear migration events are dependent on microtubules and associated motors. For example, in *Arabidopsis* root hairs, nuclear migration appears to be mediated primarily by the actin cytoskeleton (Chytilova et al., 2000).

To better understand the regulation of nuclear migration, we are studying three sets of nuclear migrations that occur during the development of *Caenorhabditis elegans*. A group of epithelial blast cells, called P cells, have nuclei on the right and left lateral sides of the newly hatched larva; these nuclei migrate ventrally to form a single row in the ventral cord (Fig. 1) (Sulston and Horvitz, 1977). The P cells later divide to produce motoneurons and epithelial cells, some of which form the vulva, the egg laying and mating organ of hermaphrodites.

During embryogenesis, left and right groups of dorsal epithelial cells intercalate, and their nuclei migrate to the contralateral side of the embryo. These cells subsequently fuse, forming a syncytium called hyp7 (Fig. 1) (Sulston et al., 1983). A third set of nuclear migrations occurs in the embryonic intestine, when the nuclei in the left and right groups of cells in the intestinal primordium move toward the future apical surface, where the intestinal lumen forms (Fig. 1) (Leung et al., 1999).

Genetic screens have identified two *C. elegans* genes, *unc-83* and *unc-84*, that function in these three sets of nuclear migrations. Mutations in these genes were originally identified because their failure in P-cell nuclear migration leads to uncoordinated movement (Unc) and vulval defects (Horvitz and Sulston, 1980; Sulston and Horvitz, 1981). *unc-84* encodes a protein of unknown function with a C-terminal SUN domain (for Sad1p, UNC-84) that is conserved from fission yeast to humans (Malone et al., 1999). UNC-84::GFP localizes to the nuclear envelope of most somatic cells in *C. elegans* (Malone et al., 1999). In *S. pombe*, the homologous protein Sad1p localizes to the nuclear envelope and spindle pole body, where it plays a role in spindle architecture (Hagan and Yanmagida, 1995).

We have analyzed the nuclear migration defects of *unc-83* mutants and extend the characterization of *unc-84* mutants. We show that neither gene appears to be necessary for centrosomes to associate with nuclei. We cloned the *unc-83* gene and found that it encodes a novel protein associated with the nuclear envelope and is expressed in cells undergoing nuclear migration. The localization of UNC-83 to the envelope is dependent on *unc-84(+)* function. Our data suggest that UNC-83 and UNC-84 interact through the SUN domain of UNC-84.

MATERIALS AND METHODS

C. elegans strains, genetics and phenotypic analysis

Bristol N2 (Brenner, 1974) was used as the wild-type *C. elegans* strain and as the parent of all mutant strains. Mutants were isolated after mutagenesis with ethyl methanesulfonate (EMS). *unc-83(ku18)* was isolated in a screen for suppressors of the multivulva (Muv) phenotype of activated *let-60(n1046)/ras* (Sundaram and Han, 1995; Wu and Han, 1994). The alleles *e1408*, *e1409*, *n320*, *n368* and *n370* were isolated in screens for egg-laying defective (Egl) mutants (Horvitz and Sulston, 1980; Trent et al., 1983). Alleles *n1727*, *n1766*, *n1826*, *n1827*, *n1866*, *n1883*, *n1886*, *n2011*, *n2012*, *n2100*, *n2101* and *n2104* were isolated in screens for suppressors of the Muv phenotype of *lin-15(n765)* (Clark et al., 1992), and *unc-83(n1497)* was found to be a suppressor of the Muv phenotype of *lin-1(e1275)* (a gift from S. Clark).

For mapping *unc-83*, the strain DA1090 (*exp-2(sa26sd) dpy-11(e224)/unc-46(e177) sDf30 V; mnDp26* – kindly provided by Leon Avery, University of Texas Southwestern, Dallas, TX) was used to create *exp-2(sa26), dpy-11(e224)/unc-83(e1408)* heterozygotes from which Dpy non-Let recombinants were picked. One of the seven such recombinants segregated *unc-83(e1408)*. In the process of mapping and cloning *unc-83*, we rescued *dpy-11(e224)* by injection of cosmid T04F11, placing *unc-83* in the small physical region between T04F11 and F12F3, which contains *exp-2* (Davis et al., 1999). Cosmids covering this region were injected with a *sur-5::GFP* plasmid as a marker (Yochem et al., 1998) to test for rescue by standard techniques (Mello et al., 1991).

Defects in P-cell migration were quantified by counting the Pn.p daughter cells of the P cells in the ventral cords of L2 hermaphrodites raised at either 15 or 25°C using a microscope equipped with Nomarski optics (Sulston and Horvitz, 1977). We scored 11 of the 12 Pn.p cells; we did not score P12.p, the most posterior of the Pn.p cells. Alternatively, P-cell migration was quantified by counting P-cell-derived GABAergic neurons using the *oxIs12(unc-47::GFP)* marker (McIntire et al., 1997), which was crossed into an *unc-83(e1408)* background. Defects in hyp7 nuclear migration were quantified by counting the number of hyp7 nuclei found abnormally, using Nomarski optics, in the dorsal cords of L1 or L2 hermaphrodites raised at 20°C. We scored all 15 hyp7 nuclei that would be present in the dorsal cord if all migrations failed (Sulston et al., 1983). Defects in nuclear migration events leading towards intestinal polarization were scored as previously described (Leung et al., 1999).

Molecular analysis of UNC-83

Subclones of W01A11 were made as follows and tested for the rescue of the hyp7 nuclear migration defect. pD19 and pD21 were made by excising a 12.2 kb *Xho*I or an 8.8 kb *Afl*II fragment, respectively, and re-ligating the W01A11 backbone. pD22 was constructed by ligating a 10.5 kb fragment of W01A11 from a *Eag*I, *Hpa*I double digest into the *Eag*I and *Eco*RV sites of pBS (Stratagene, La Jolla, CA).

Expressed sequence tags (ESTs) were identified from the predicted open reading frame using The Intronerator software (Kent and Zahler, 2000). ESTs were kindly provided by Yuji Kohara (National Institute of Genetics, Mishima, Japan). The sequences of the cDNAs represented by ESTs yk230e1 and yk629c11 were determined.

dsRNA for RNAi experiments was made from a PCR product template with overhanging T7 promoters using T7 RNApol and injected into N2 adult hermaphrodites (Fire et al., 1998). L2 worms were scored for hyp7 and P-cell nuclear migration defects as described above 43-45 hours after injection. The 5′ RNAi experiment was directed against yk230e1 sequence corresponding to exons 3 through 7. The 3′ RNAi experiment was directed against exons 8 through 16.

Antibodies and immunofluorescence

Part of UNC-83, from the ATG of the short transcript in exon 8 to the beginning of the predicted transmembrane domain, was amplified by *Pfu* polymerase (Stratagene, La Jolla, CA) with appropriate overhanging restriction sites and cloned in-frame into the *Bam*HI and *Sma*I sites in pGEX-2T (Amersham Pharmacia Biotech, Piscataway, NJ) to create a construct encoding an UNC-83/GST fusion protein or into the *Bam*HI and *Pst*I sites of pMAL-c2 (New England Biolabs, Beverly, MA) to create a construct encoding an UNC-83/MBP fusion protein. Both fusion proteins were expressed in *E. coli* strain BL21 codon plus (Stratagene) and purified on either glutathione sepharose 4B beads (Amersham Pharmacia Biotech) or amylose resin (New England Biolabs), according to the protocol supplied by the manufacturers.

Monoclonal antibodies were raised in six-week-old BALB/c female mice (Jackson Laboratories, Bar Harbor, ME). Six mice were injected three times at three week intervals with approximately 100 μg of the UNC-83/MBP fusion protein. One week after the last boost, test bleeds were examined against the UNC-83/GST fusion protein. The spleen was removed from the best responder 3 days after a final boost. The B cells were fused to a FOX-NY mouse myeloma at the University of Colorado Cancer Center tissue culture core facility (Denver, CO). 72 hybridoma clones were found to recognize UNC-83/GST by ELISA and further screened by immunofluorescence. Subclones of nine positive hybridomas were screened by immunofluorescence, and line 1209D7 was chosen as the best hybridoma based on a high signal-to-background noise ratio. All monoclonal antibodies were collected as tissue culture supernatants in RPMI + 15% fetal bovine serum. UNC-83 was not recognized on western blots using these antibodies; against whole wild-type or *unc-*

83 null *C. elegans* extracts, using 12 different monoclonal antibodies, western blots were blank (data not shown). Either levels of UNC-83 were too low to be detected in whole worm extracts, or the monoclonal antibodies failed to recognize denatured UNC-83 on a western blot. The antibody did recognize overexpressed UNC-83/GST fusion protein on a western blot.

The UNC-84::GFP line has bee described previously (Malone et al., 1999); it was detected with GFP polyclonal antibody (Clontech, San Francisco, CA). The mouse monoclonal antibody IFA was used to detect embryonic centrosomes (Leung et al., 1999; Pruss et al., 1981). The rabbit polyclonal antibody against the *C. elegans* lamin homolog (Liu et al., 2000) was kindly provided by Y. Gruenbaum (The Hebrew University, Jerusalem, Israel). The anti-lamin antibody was used at a 1/250 dilution in PBST. A JAM-1::GFP line was made by integrating pJS191 (Raich et al., 1999) into N2 lines creating *kuIs47* and crossed into an *unc-83(e1408)* background to identify adherens junctions.

For immunofluorescence with the UNC-83 antibody, embryos were extruded from slightly starved hermaphrodites, permeabilized by the freeze-crack method, fixed for 10 minutes in –20°C methanol, air dried and blocked in PBST (phosphate-buffered saline + 0.1% Triton X-100) +5% dry milk (Miller and Shakes, 1995). The fixed specimens were stained as described (Miller and Shakes, 1995). Primary antibody 1209D7 was used undiluted. Cy3-conjugated goat anti-mouse IgG and Cy2-conjugated goat anti-rat or anti-rabbit IgG (Jackson ImmunoResearch, West Grove, PA) diluted 1/200 in PBST were used as secondary antibodies. DNA was visualized by a 5 minute stain in 100 ng/ml of 4,6-diamidino-2-phenylindole (DAPI; Sigma, St Louis, MO) in PBST.

Images were collected using an Axioplan2 microscope (Carl Zeiss, Thorton, NY) and a Hamamatsu C4742-95 CCD camera (Hamamatsu Photonics KK, Bridgewater, NJ). Images were deconvolved and analyzed using Openlab 2.0.7 (Improvision, Lexington, MA) software, and figures were compiled using Photoshop 6.0 (Adobe, San Jose, CA), or as described (Leung et al., 1999).

GST pulldown assays

The conserved SUN domain of UNC-84 (the C-terminal 198 amino acids) was amplified by PCR with appropriate overhanging restriction sites, cloned into the *Bam*HI and *Eco*RI sites of pGEX-2T to create UNC-84-SUN/GST, and purified on glutathione sepharose 4B beads as described above. Alternatively, pGEX-2T was used alone to express GST. Crude extracts containing soluble UNC-83/MBP fusion protein were prepared as above. [^{35}S]methionine-labeled UNC-83 was made using the TnT-coupled reticulocyte lysate system (Promega, Madison, WI). The UNC-83B transcript, as represented by the EST yk230e1, was used as the template. The pulldown assay was preformed in a crude *E. coli* BL21 extract in PBS + 10% glycerol as previously described (Melcher and Johnston, 1995). Relative amounts of [^{35}S]methionine-labeled UNC-83 were detected and quantitated using a Storm PhosphorImager and ImageQuant software (Amersham Pharmacia Biotech).

RESULTS

Mutations in *unc-83* disrupt three sets of nuclear migrations

In addition to the original *unc-83(e1408)* mutation, 18 other *unc-83* alleles have been collected from various screens; many were isolated as suppressors of the multivulva phenotype caused by mutations that abnormally activate the Ras pathway in vulval development (see Materials and Methods). For each of these 19 alleles, we examined nuclear migration for the P cells and the precursors of hyp7 cells; representative alleles were also examined for nuclear migration in the intestinal primordium. We also examined pronuclear migration in newly fertilized *unc-83(e1408)* embryos and found the migration to be completely normal when compared with wild-type (data not shown).

P cell nuclear migrations often failed in *unc-83* mutants. Nuclear migration for the P cells was quantified by counting Pn.p cell nuclei in the ventral cords of second larval stage (L2) hermaphrodites using Nomarski optics. A strong temperature-sensitive phenotype was observed for all *unc-83* alleles similar to that reported for *unc-83(e1408)* animals (Table 1) (Sulston and Horvitz, 1981). While 90% of P cell nuclei migrated to the proper ventral position (termed the ventral cord) at 15°C, only 30-50% of the nuclei migrated to the ventral cord at 25°C. As most of these alleles probably eliminate *unc-83* function , it is unlikely that the *unc-83* gene product is thermolabile. Rather, our results support the hypothesis of Sulston and Horvitz (Sulston and Horvitz, 1981) that the process of P cell nuclear migration is intrinsically temperature-sensitive in the absence of *unc-83* function.

The final positions of the P-cell nuclei depend on migrations of the P cells in addition to nuclear migrations within the P cells. Sulston and Horvitz have reported that P cells generally die in *unc-83* mutant animals if their nuclei fail to migrate to the ventral cord (Sulston and Horvitz, 1981). By contrast, mutations in *unc-73* or *let-502* disrupt P cell migration before nuclear migration. In these mutants, the P cells survive and develop in lateral positions. To determine if P cells can develop laterally in *unc-83* mutants, we scored P cell nuclear migration using an *unc-47::GFP* fusion gene, which is normally expressed in the 19 GABAergic neurons of the ventral cord (McIntire et al., 1997). Of these 19 GFP-positive cells, 13 are derived from P cells. In the wild type, all 19 cells were present (see Fig. 1B; *n*=15 worms). However, in *unc-83(e1408)* hermaphrodites raised at 25°C, we observed only 12.3 (±1.8) UNC-47::GFP-positive cells (Fig. 1C; *n*=16). In contrast to *unc-73* and *let-502* mutants, in which UNC-47::GFP-expressing neurons survive and develop in a lateral position (A. Spencer, C. J. M., M. H., unpublished), we did not observe any lateral UNC-47::GFP marked neurons in *unc-83(e1408)* worms.

We also examined the embryonic nuclear migrations of the precursors of the hyp7 hypodermal syncytium. Most *unc-83* alleles caused the hyp7 nuclei to accumulate in a central region along the dorsal cord, rather than undergo the normal migration to contralateral positions. We counted hyp7 nuclei in the dorsal cords of L1 hermaphrodites using Nomarski optics. As the hyp7 nuclear migration defect is not temperature sensitive (Sulston and Horvitz, 1981), we scored worms raised at 20°C (Table 1; Fig. 1D-F). Twelve *unc-83* mutants were severely abnormal in hyp7 nuclear migrations, one displayed an intermediate phenotype, and in six mutants hyp7 nuclei migrated normally (Table 1).

Nuclear migration was scored in the intestinal primordia of *unc-83(e1408)* and *unc-83(ku18)* animals. Both mutants had strong migration defects as indicated by nuclei not at the midline (future apical region) of the primordium at both 25°C and 15°C (Table 2; Fig. 1H-I). Surprisingly, mutant embryos raised at 25°C had slightly less severe defects than embryos raised at 15°C, in contrast to the effect of temperature on P-cell nuclear migrations. In some strains, the defect appeared to get worse as development progressed from the pre-bean to the

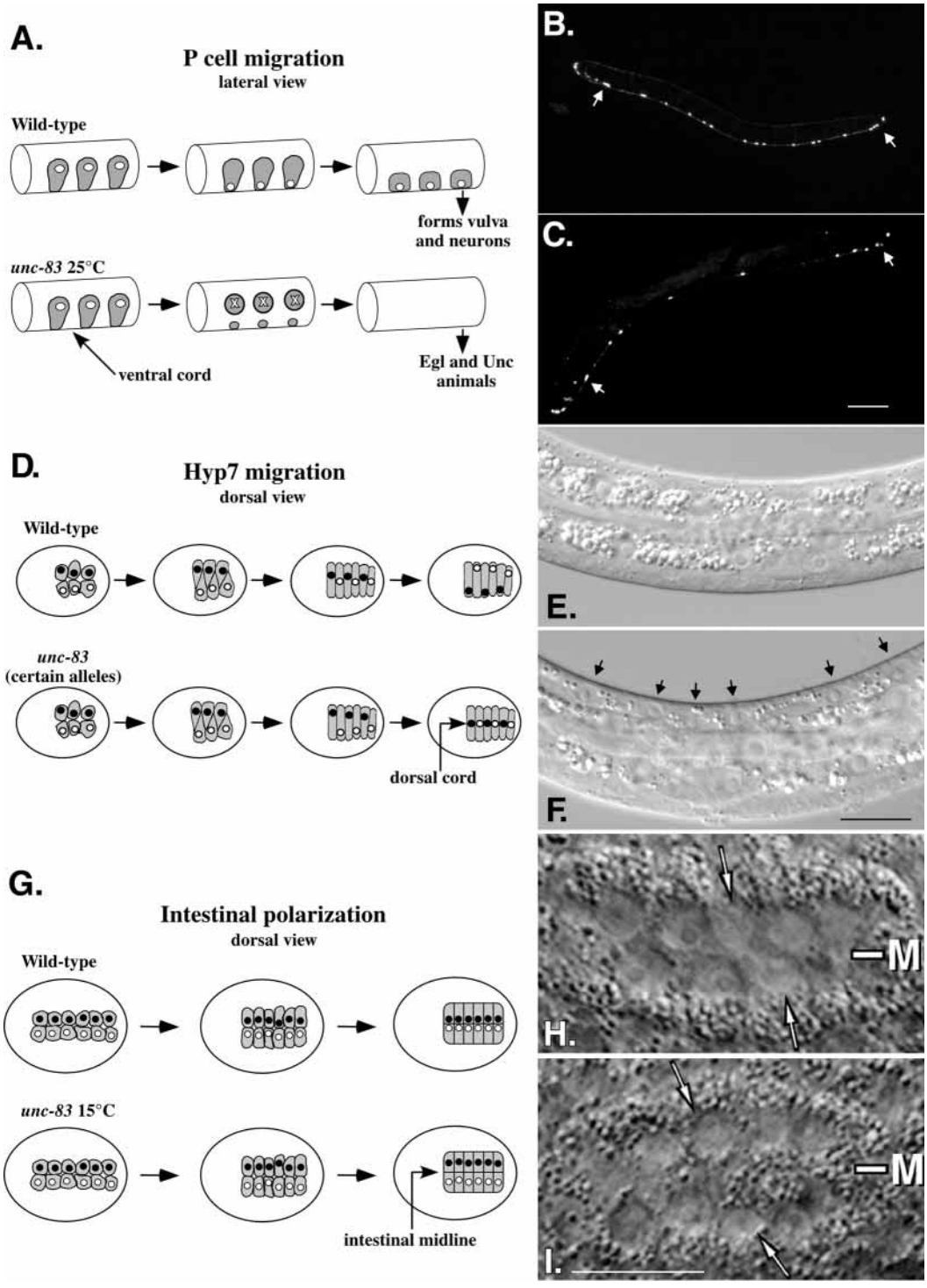

Fig. 1. *unc-83* mutations disrupt the nuclear migrations of three cell types. (A) Left lateral view of P-cell nuclear migration in wild-type and *unc-83* embryos at 25°C. P-cell cytoplasm is gray and nuclei are white. White X marks dying nuclei. Ventral is downwards. (B-C) Expression of UNC-47::GFP in GABAergic neurons in the ventral cords of adult hermaphrodites. Ventral is downwards, anterior is leftwards. (B) Wild type, showing the 19 neural cell bodies scored between the arrows. (C) *unc-83(e1408)*, with only 11 GABAergic neurons between the arrows. (D) The dorsal surface of a pre-elongation embryo illustrating intercalation and nuclear migration of hyp7 precursors in wild-type and *unc-83* embryos. Cytoplasm of the hyp7 precursors is gray, nuclei that migrate from right to left are black, and nuclei that migrate from left to right are white. Anterior towards left, right is upwards. (E,F) Lateral view of L1 hermaphrodites. Dorsal is upwards. (E) Wild type showing no nuclei in the dorsal cord. (F) An *unc-83(e1408)* hermaphrodite. The arrows mark misplaced hyp7 nuclei in the dorsal cord. (G) A dorsal view, through the middle of a pre-elongation embryo, of nuclear migration during intestinal polarization during the E16 stage in wild-type and *unc-83* embryos raised at 15°C. Cytoplasm of embryonic intestinal cells is gray, nuclei right of the midline are black and nuclei left of the midline are white. Anterior is leftwards, right is upwards. (H) Wild-type embryonic intestinal cells. (I) *unc-83(e1408)* embryonic intestinal cells. M marks the midline where the intestinal lumen will form, the arrows mark examples of intestinal nuclei at the mid-line in wild-type and separated away from the midline in the *unc-83(e1408)* embryo. Scale bars: 100 μm for B,C; 10 μm for E,F; 10 μm for H,I.

bean stage. Perhaps *unc-83* is required for nuclear positioning near the midline after migration. The intestinal cells defective in nuclear migration did not show the wild-type polarized distribution of cytoplasmic materials such as yolk and lipid vesicles. Nonetheless, the intestine developed an apical lumen, which functioned in feeding during larval development.

Mutations in *unc-83* do not disrupt centrosome attachment to the nuclear envelope, the structure of the nuclear matrix, or microtubule distributions

Several models for directed nuclear migration require that centrosomes associate with nuclei (Malone et al., 1999; Morris, 2000; Raff, 1999). Thus, defects in nuclear migration could

Table 1. Nuclear migration defects of *unc-83* mutant alleles

unc-83 allele	% of cell nuclei that migrated normally±s.d.* P cell (25°C)†	P cell (15°C)†	hyp7 cells‡
Wild type	100±0	100±0	100±0
n1883	39±15	95±5	7±8
n1866	47±23	92±7	8±6
e1409	34±13	91±7	9±6
n370	49±23	97±4	11±7
n1727	33±9	95±5	12±9
n2104	30±14	89±7	13±10
n2101	36±9	87±9	13±9
e1408	39±10	93±4	13±9
n2100	41±13	90±8	13±8
n1886	35±10	90±7	14±8
n1826	29±15	94±6	16±9
n1497	59±14	97±4	17±9
n2011	36±12	92±7	60±16
n2012	36±20	93±7	98±4
n320	51±15	97±4	99±2
n368	39±12	91±6	100±1
n1766	56±13	97±4	100±0
ku18	35±12	95±6	100±1
n1827	35±15	90±7	100±1

*Standard deviation is a worm-to-worm variation.
†Sample size was at least 10 worms.
‡Sample size was at least 20 worms.

Table 2. Embryonic intestinal nuclear migration defects

unc-83 allele	Stage*	Temperature	% of intestinal nuclei not localized at the midline	*n*
Wild type	Pre-bean	15°C	12	49
	Bean	15°C	0	41
	Pre-bean	25°C	12	35
	Bean	25°C	0	54
e1408	Pre-bean	15°C	100	42
	Bean	15°C	97	34
	Pre-bean	25°C	34	38
	Bean	25°C	83	58
ku18	Pre-bean	15°C	100	27
	Bean	15°C	100	24
	Pre-bean	25°C	87	38
	Bean	25°C	100	36

*Pre-bean stage is before the onset of elongation, and the bean stage is shortly after elongation has begun. Both are during the E16 stage.

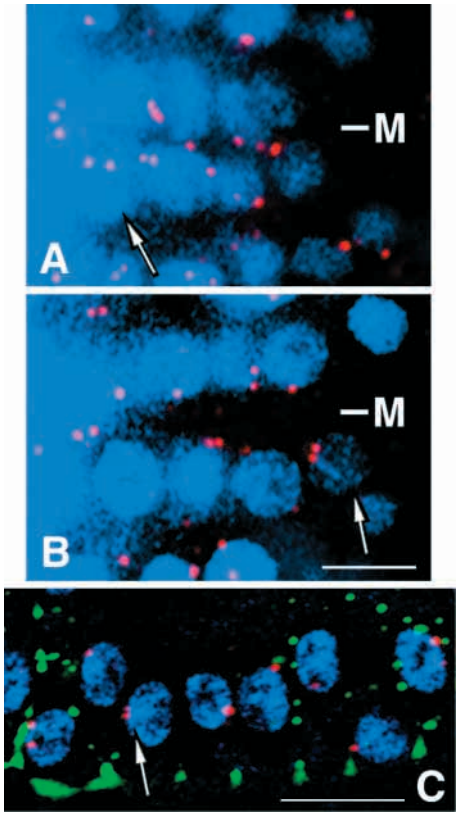

Fig. 2. *unc-83* mutations do not disrupt centrosome attachment to the nucleus. Dorsal views through the intestinal primordium (A,B) or through hyp7 precursors (C) in pre-elongation embryos grown at 15°C. Anterior is leftwards. (A) Wild-type embryo. (B,C) *unc-83(e1408)* embryos. Embryos were stained with the IFA antibody to identify centrosomes (pseudocolored red) and DAPI to identify chromatin (pseudocolored blue). hyp7 precursors were identified using the *jam-1::GFP* marker to show hypodermal cell boundaries, pseudocolored green. M marks the midline where the intestinal lumen will form. The arrows mark examples of nuclei with centrosomes properly associated. Note that for the wild-type embryo, nuclei have migrated toward the midline, but nuclei are separated away from the midline in the *unc-83(e1408)* embryo. Because of the limited focal plane of these images, only a subset of nuclei or centrosomes are shown. Scale bars: in B, 5 μm for A,B; in C, 5 μm for C.

result from defects in the association of centrosomes with nuclei. In the wild-type intestinal primordium, centrosomes are closely juxtaposed to the intestinal nuclei. The centrosomes are initially adjacent and either anterior or posterior to nuclei. However, before or during nuclear migration, centrosomes in the majority of intestinal cells rotate 90° to face near the midline of the intestinal primordium (Leung et al., 1999). We examined the distribution of centrosomes in the intestinal primordia of *unc-83(e1408)* mutants and found that centrosomes appeared to be associated with nuclei in all of the intestinal cells examined. Moreover, the centrosomes appeared to reposition toward the midline (Table 3; Fig. 2A-B). Thus, centrosomal re-positioning does not require nuclear migration. We also examined the distribution of centrosomes of the hyp7 cells in *unc-83* mutants and found that centrosomes were associated normally with migrating nuclei (Fig. 2C). These data suggest that UNC-83 is not required at the nuclear envelope for centrosome attachment.

The nuclear matrix, composed of lamin and associated proteins, has been proposed to play an important structural role in nuclear migration (Gruenbaum et al., 2000). We examined lamin localization by immunofluorescence during hyp7 nuclear migration in wild-type and *unc-83(e1408)* embryos. Lamin appeared to be localized normally in *unc-83(e1408)* embryos (Fig. 3), suggesting that *unc-83* is not essential for maintaining the gross structure of the nuclear matrix during nuclear migration.

Microtubules and the associated motor dynein also play important roles in many nuclear migration events (Gonczy et al., 1999; Mosley-Bishop et al., 1999; Reinsch and Gonczy, 1998). We therefore examined the distribution of microtubules in the intestinal primordium of *unc-83(e1408)* embryos. In all

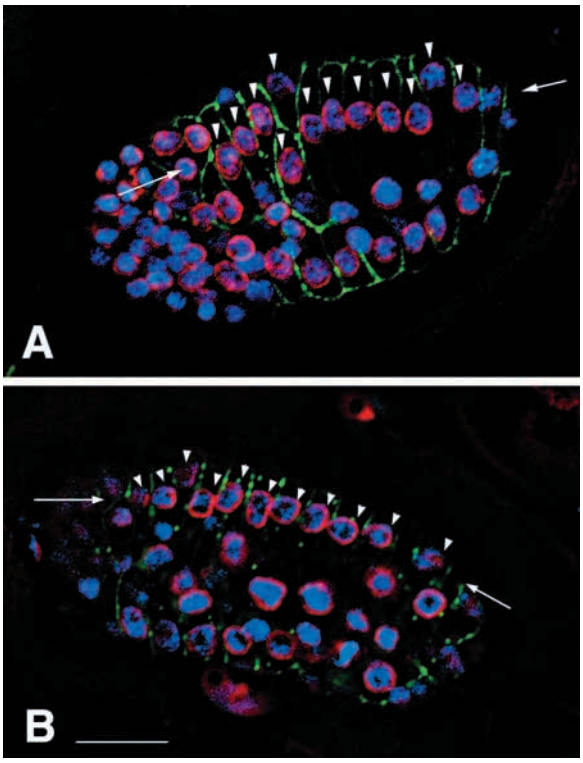

Fig. 3. *unc-83* mutations do not disrupt the gross structure of the nuclear lamina. (A) Dorsolateral view of a wild-type embryo. (B) Lateral view of an *unc-83(e1408)* embryo. Anterior is leftwards. Both embryos are in a JAM-1::GFP background to stain hypodermal adherens junctions, colored green. Embryos were stained with an anti-Lamin antibody to identify the nuclear lamina (pseudocolored red) and DAPI to identify chromatin (pseudocolored blue). Arrows mark the dorsal midline. Arrowheads identify hyp7 nuclei. Scale bar: 10 μm.

cases (n>25), microtubules were arranged as previously described for wild type (data not shown) (Leung et al., 1999). Of course *unc-83* could be disrupting microtubule dynamics in a more localized pattern that we were unable to detect in the small cells in which nuclear migration events take place. Unfortunately, we were unable to examine the behavior of dynein heavy chain in *unc-83* mutant cells during nuclear migration events, owing to their small size and high levels of cytoplasmic staining. However, dynein heavy chain was observed to be properly localized at the nuclear envelope in *unc-83(e1408)* early embryos and adult gonad cells (data not shown).

Multiple *unc-83* transcripts encode novel transmembrane proteins

To better understand the role of *unc-83* in nuclear migration, we cloned *unc-83*. *unc-83* was originally mapped on chromosome V near *dpy-11* (Horvitz and Sulston, 1980). We further mapped *unc-83* to a narrow region between *exp-2* and *dpy-11* (Fig. 4A; see Materials and Methods). Cosmids in this region were injected and tested for their abilities to rescue the nuclear migration defects of *unc-83(e1408)* mutants. Cosmid W01A11 completely rescued the *unc-83(e1408)* nuclear migration defect of embryonic hyp7 cells. Large deletions in W01A11 were constructed and rescue results implicated an 11 kb region of W01A11 (Fig. 4B). Finally, a 10 kb subclone of W01A11 containing a single predicted open reading frame (W01A11.3) was found to rescue the hyp7 nuclear migration defect (Fig. 4B). However, we were never able to rescue the P-cell nuclear migration defect, even after injecting both W01A11 and the upstream cosmid ZK40.

Table 3. Centrosome positions in the intestinal primordium

Genotype	% of cells in which centrosomes were properly oriented*	*n*
Wild type	83	214 (14 embryos)
unc-83(e1408)	76	232 (15 embryos)
unc-84(n369)	73	232 (15 embryos)

*All embryos were raised at 15°C and scored for centrosome positions at the E16 stage (pre-bean stage). In all cases, centrosomes were located adjacent to the nucleus. Nuclei in which both centrosomes were positioned on the midline facing half of the nucleus were scored as oriented. Those nuclei where one or both centrosomes were on the opposite half of the nucleus were scored as not oriented.

We have detected three UNC-83 transcripts, UNC-83A, UNC-83B and UNC-83C, which encode proteins predicted to contain 1042, 974 and 741 residues, respectively (Fig. 4C). These proteins share a common 741 residue C terminus. UNC-83A and UNC-83B were identified by ESTs using The Intronerator software (Kent and Zahler, 2000). The cDNA yk629c11 (Kohara, 1996) represents UNC-83A. This cDNA is likely to contain the entire open reading frame, as an in-frame stop codon was detected 5′ to the first ATG. The UNC-83B transcript is defined by cDNA yk230e1 (Kohara, 1996). The 5′ end of yk230e1 contains part of an SL1 *trans*-spliced leader sequence which is spliced to the 5′ end of a majority of *C. elegans* transcripts (Huang and Hirsh, 1989), suggesting that we have identified the 5′ end of UNC-83B. The 5′ end of the UNC-83C transcript was isolated using PCR from a mixed stage λgt11 library (Okkema and Fire, 1994), with primers against an SL1 sequence and exon 10. This PCR product represents the complete 5′ end because it includes an SL1 leader sequence. We do not know if other UNC-83 transcripts exist.

All three of the identified UNC-83 transcripts extend at their 5′ ends beyond the genomic region covered by the minimal rescuing fragment pD22 (Fig. 4). This observation suggests that there may be additional *unc-83* transcripts that start 3′ of the start of *unc-83C* or that another promoter is used to initiate transcription, possibly in the intron between exons 7 and 8.

To confirm that the *unc-83A*,*unc-83B* and *unc-83C* transcripts are responsible for *unc-83* gene function, we determined the sequences of the open reading frames of 19 *unc-83* mutants. We identified molecular lesions in 16 *unc-83* alleles. All of the identified molecular lesions are severe, introducing a premature stop codon, mutating a splice site or, in one case, deleting 138 base pairs, which puts the rest of the protein out-of-frame (Fig. 4D). We did not identify lesions in the alleles *n368*, *n2011* or *n1727*, suggesting that these mutations lie in the promoter or introns of *unc-83*.

The 16 identified *unc-83* molecular lesions fall into two classes based on the severity of their hyp7 cell nuclear

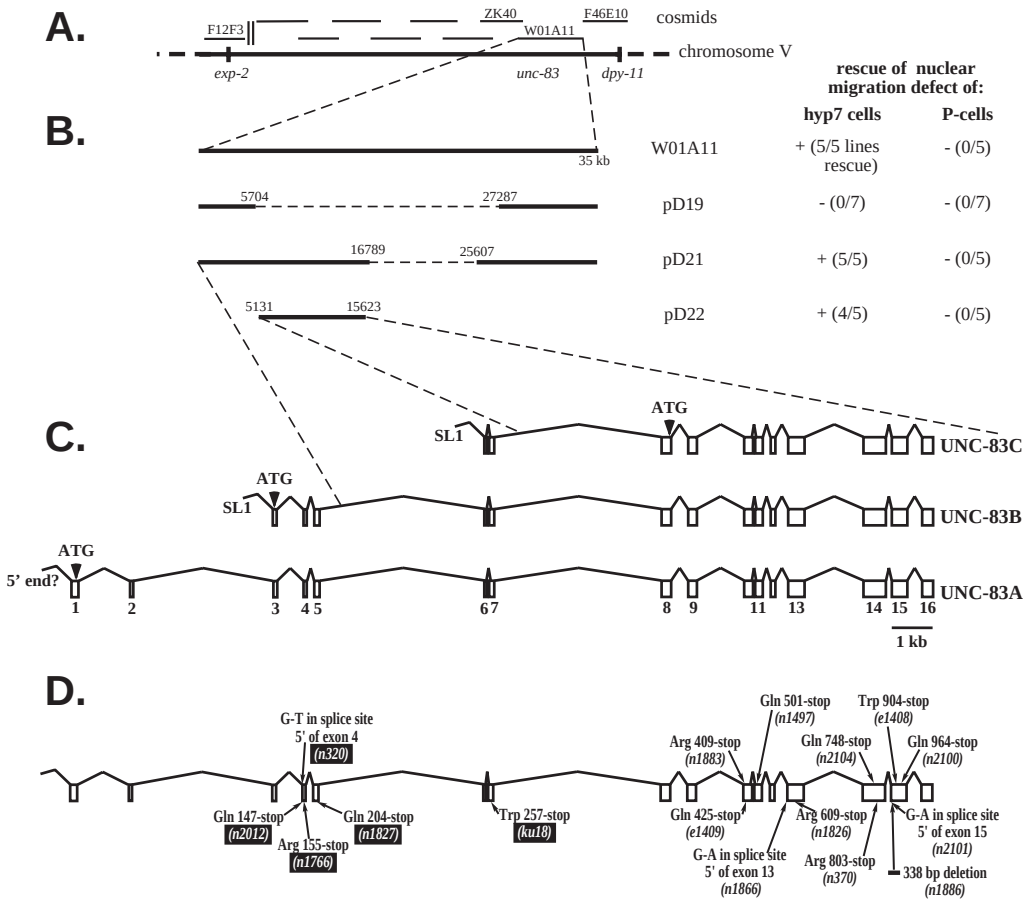

Fig. 4. Cloning *unc-83*. (A) The genomic region on chromosome V between *exp-2* and *dpy-11* is shown. The names of cosmids in the region that rescue *exp-2* or *dpy-11* or that contain part of *unc-83* are indicated. (B) Cosmid W01A11 and its derivatives are shown on the left. The deleted parts of W01A11 in pD19 and pD21 are indicated by broken lines. The numbers above the lines are the sites of breakpoints of the deletions of W01A11 in pD19 and pD21 and of the region of W01A11 subcloned into pBS to create pD22 (see Materials and Methods). On the right are data concerning the rescue of the *unc-83(e1408)* nuclear migration defect of hyp7 cells and P cells. (C) The genomic regions of three predicted transcripts of *unc-83* are shown. The white boxes represent exons, which are connected by introns. The predicted translational start site (ATG) in each transcript and any detected SL1 splice leader sequences of each transcript are indicated. The numbers at the bottom label exons 1 to 16 of the longest *unc-83* transcript. (D) The molecular lesions of 16 *unc-83* alleles are shown. The arrows indicate the approximate sites of the lesions. For nonsense mutations, the affected amino acid is numbered. Black boxes indicate alleles that did not disrupt hyp7 nuclear migration, while a white background indicates alleles that disrupted both P cell and hyp7 nuclear migrations. Sequence data for the *unc-83* transcripts are available from GenBank/EMBL/DDBJ under Accession Number AF338767.

migration defects (see Table 1). The *unc-83* alleles that lead to normal hyp7 nuclear migration, *n2012*, *n320*, *n1766*, *n1827* and *ku18*, have molecular lesions that disrupt the open reading frames of UNC-83A and UNC-83B, but not UNC-83C. The alleles that disrupt hyp7 nuclear migration, *n1883, e1409*, *n1866*, *n1497*, *n1826*, *n370*, *n2104*, *n1886*, *n2101*, *e1408* and *n2100*, have molecular lesions predicted to disrupt all three UNC-83 open reading frames. This result suggests that the shorter UNC-83C transcript is sufficient for hyp7 nuclear migration. Furthermore, as all alleles disrupt P cell nuclear migration (see Table 1), and both alleles tested (*e1408* and *ku18*) disrupt intestinal nuclear migration, we propose that at least one of the longer UNC-83A or UNC-83B transcripts is necessary for P-cell and intestinal nuclear migration.

To examine further the tissue specificities of the different transcripts, we performed two RNAi experiments. RNAi directed against exons 8 to 16, which should disrupt all UNC-83 products, caused strong nuclear migration defects of both P cells and embryonic hyp7 cells (Table 4). By contrast, RNAi directed against exons 3 to 7, predicted to disrupt the open reading frames of UNC-83A and UNC-83B, produced a strong P-cell nuclear migration defect but no hyp7 nuclear migration defect (Table 4).

No proteins of high similarity to UNC-83 have been identified in BLAST searches with UNC-83 sequences. In addition, no obvious homologs have been found in the complete or nearly complete genomes of yeast, *Drosophila* or humans. Thus, UNC-83 is not obviously conserved at a

Table 4. Effects of *unc-83* RNAi on nuclear migration

	% normally migrated nuclei±s.d.	
	P cell (25°C)*	hyp7 cells*
RNAi (exons 3-7)	44±16	96±5
RNAi (exons 8-16)	43±16	7±6

*At least 25 worms were scored.

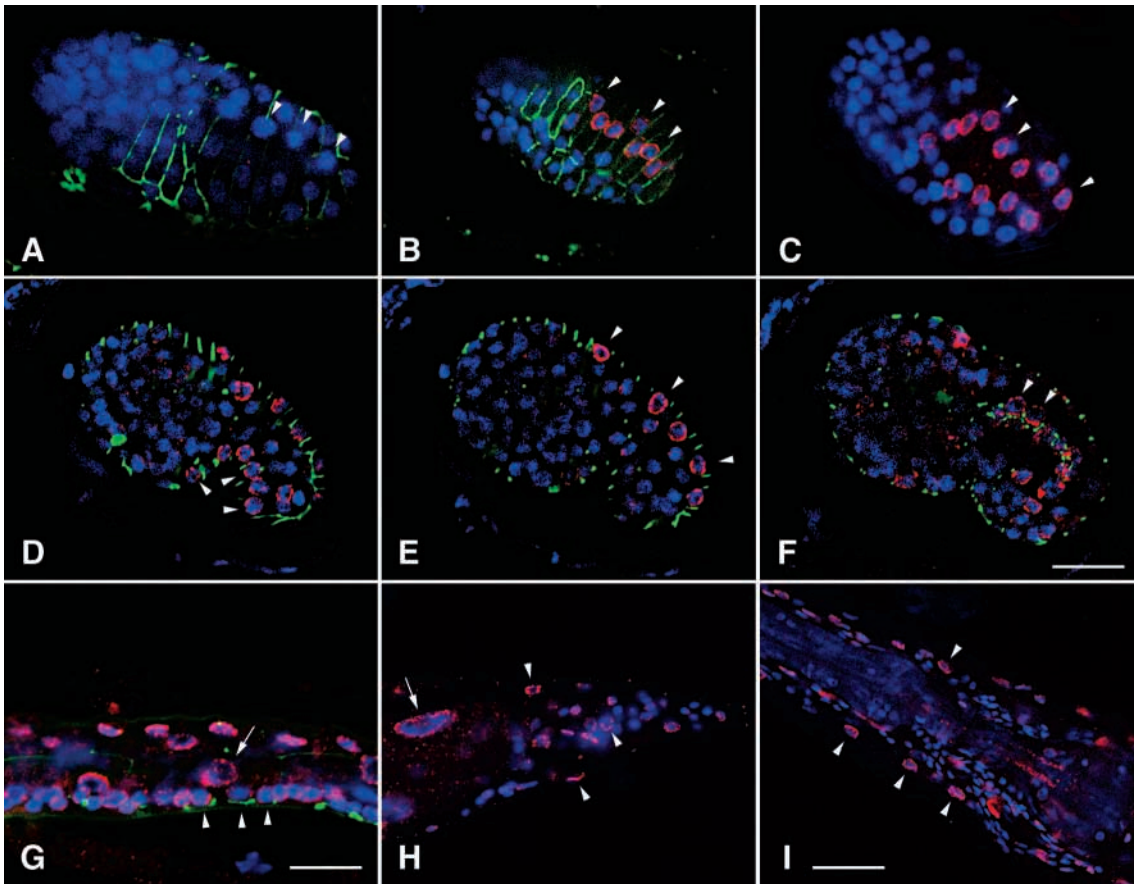

Fig. 5. UNC-83 is localized to the nuclear envelope. In all panels, anterior is leftwards, and dorsal is upwards. UNC-83 antibody localization is pseudocolored red, and DAPI staining is in blue. In some panels, JAM-1::GFP is used to show adherens junctions in green. (A-C) Pre-elongation embryos, examples of hyp7 nuclei are marked with arrowheads. (A) *unc-83(e1408)*, a putative null. (B) Wild-type. (C) *unc-83(ku18)*, an allele in which hyp7 nuclear migration is not disrupted. (D-F) Lateral views of sections through a single wild-type embryo at the onset of elongation (bean stage). (D) A section near the top with P-cell nuclei marked by arrowheads. (E) A section 1 μm lower showing hyp7 nuclei marked with arrowheads. (F) A section 4 μm lower showing UNC-83 staining in intestinal cells marked with arrowheads. (G-I) Wild-type worms. (G) A lateral view of a hermaphrodite late in the first larval stage showing UNC-83 in marked P cells. The arrow marks an intestinal cell in the same plane. (H) The tail of an adult worm. UNC-83 stained many hypodermal cells, examples are marked with arrowheads, a large intestinal cell (arrow) and other unidentified cells. (I) The head of an adult worm showing UNC-83 staining in hypodermal (examples marked with arrowheads) and other unidentified cells. Scale bars: in F, 10 μm for A-F; in G, 9 μm for G; in I, 25 μm for H,I.

sequence level, although it might be conserved at a structural level or with a similarity too low to be detected with current search tools. The only possible motifs we found in the UNC-83 sequence are a predicted transmembrane domain five residues from the C terminus (residues 1019-1037 of UNC-83A) and a short stretch of possible coiled-coil structure (residues 786-818 of UNC-83A).

UNC-83 localizes to the nuclear membranes of a subset of nuclei

To determine the subcellular localization of UNC-83, we raised monoclonal antibodies against a maltose-binding protein fusion protein containing most of UNC-83 (from the initiator methionine of UNC-83C to just before the carboxyl predicted transmembrane domain). The immunostaining patterns described below were not present in putative null *unc-83* mutants and thus are specific for the UNC-83 protein (Fig. 5A).

Antibodies against UNC-83 stained the nuclear envelopes of migratory nuclei and several additional nuclei (Fig. 5, Fig. 6). UNC-83 co-localized with two other proteins of the nuclear envelope, UNC-84 and lamin (Fig. 6) (Liu et al., 2000; Malone et al., 1999). UNC-83 has a more punctate staining pattern than Lamin. We do not know what this staining pattern correlates to, but it is unlikely to be nuclear pores since staining with a nuclear pore marker (mAb414; Covane, Richmond, CA) is even more punctate (data not shown). We were unable to co-stain with both UNC-83 and nuclear pores, because both antibodies were raised in mice. It also appears that UNC-83 is more punctate that UNC-84 (Fig. 6). This may simply be due to the fact that UNC-84 was detected as a GFP fusion protein that is likely to be overexpressed (Malone et al., 1999).

Unlike UNC-84 and lamin, which can be detected at the nuclear envelope in nearly all cells, UNC-83 was detected in only a subset of cells. UNC-83 was not detected at the nuclear envelope of migrating pronuclei. We first detected UNC-83 at the nuclear envelopes of migrating embryonic hyp7 nuclei (Fig. 5B), consistent with the onset of the first observable *unc-83* mutant defect. Later, at the bean stage of embryonic

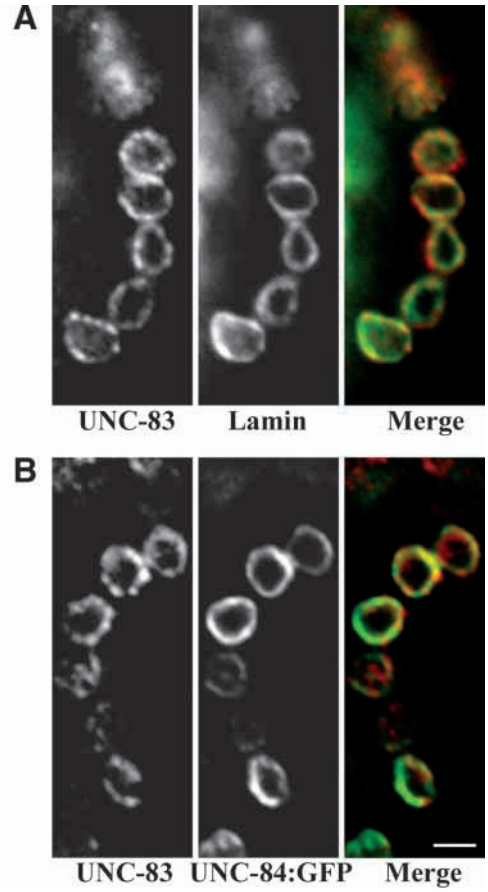

Fig. 6. UNC-83 co-localization with Lamin and UNC-84. (A) Co-localization of UNC-83 (left panel) and Lamin (center panel) shown merged together (right panel) with UNC-83 pseudocolored red and Lamin in green. (B) Co-localization of UNC-83 (left panel) and UNC-84::GFP (center panel) shown merged together (right panel) with UNC-83 pseudocolored red and UNC-84::GFP green. Scale bar: 2 μm.

development, UNC-83 was localized to the nuclear envelopes of hyp7 cells, P cells and intestinal cells (Fig. 5D-F). By the comma stage, UNC-83 was detected in these cells as well as in several additional cells in the pharynx. *unc-83(ku18)* mutants, which have nuclear migration defects in the P cells and the intestinal cells but not in hyp7 precursors, showed immunostaining for UNC-83 in the hyp7 nuclei but not in the P cell nuclei or intestinal nuclei (Fig. 5C). In late stages of wild-type embryos, and in larvae and adults, UNC-83 was detected on nuclei in a wide variety of cells, including several cells around the pharynx and in the uterus.

UNC-84 likely recruits UNC-83 to the nuclear membrane

Several of the nuclear migration defects of *unc-83* mutants appeared very similar to those described previously for *unc-84* mutants, and at least some of the migration defects did not appear to be exacerbated in *unc-83; unc-84* double mutants (Malone et al., 1999). These results, together with the observation that UNC-83 and UNC-84 colocalize, suggest that these proteins could function in the same pathway or complex to control nuclear migration. We therefore examined the localization of UNC-83 in a collection of *unc-84* mutant

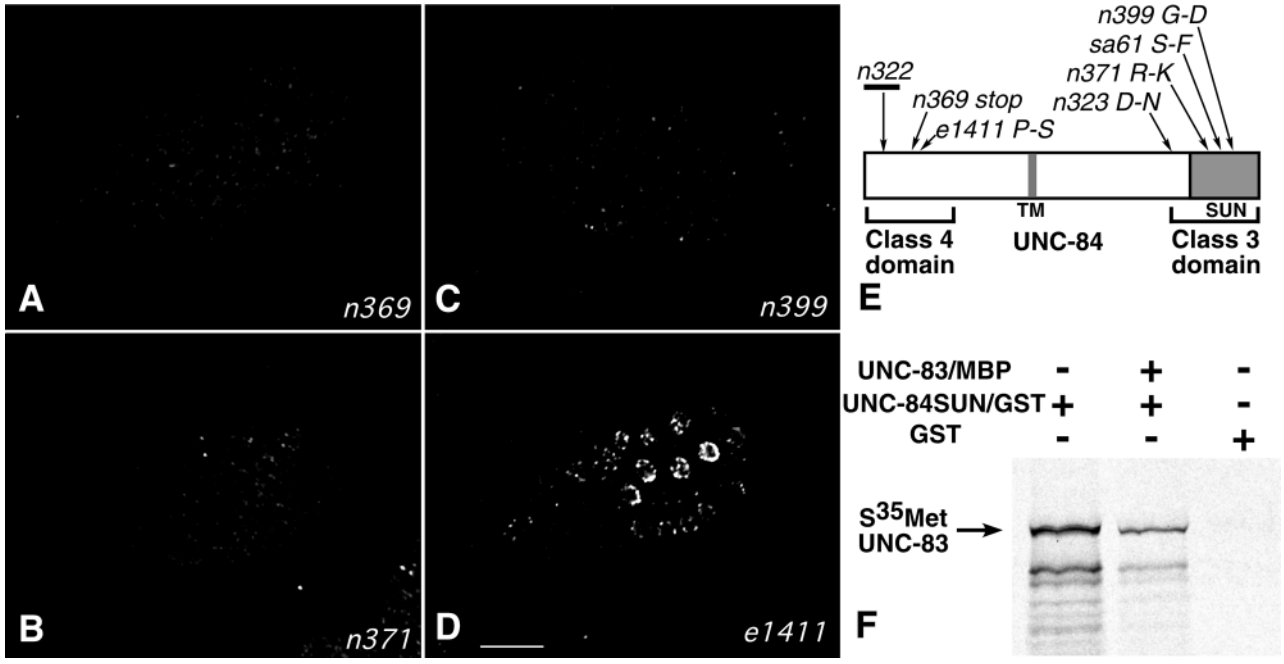

Fig. 7. UNC-84 is required to target UNC-83 to the nuclear envelope. (A-D) Localization of UNC-83 antibody in pre-elongation embryos in the four classes of *unc-84* embryos. Anterior is leftwards. (A) *unc-84(n369)*, a class 1 or null allele. (B) *unc-84(n371)*, a class 2 allele. (C) *unc-84(n399)*, a class 3 allele. (D) *unc-84(e1411)*, a class 4 allele. Scale bar: 10 μm. (E) The molecular lesions in UNC-84 of the seven alleles tested for UNC-83 localization. Only one allele from each class is shown in A-D, although other alleles were tested (see text). (F) UNC-83 and the SUN domain of UNC-84 interact in vitro. The ^{35}S-methionine-labeled UNC-83 that was pulled down by the bait-coated beads is shown. Labels designate the GST fusion protein attached to beads used as bait, or the presence of cold UNC-83/MBP in the middle lane.

animals (Fig. 7E). We found that UNC-83 failed to localize to the nuclear envelope in the null mutant *unc-84(n369)* and in class 2 and 3 *unc-84* alleles *n323*, *n371*, *sa61* and *n399*, which have missense mutations in the conserved C terminus SUN domain of UNC-84 (Fig. 7A-C) (Malone et al., 1999). By contrast, UNC-83 was detected at the nuclear envelope in class 4 *unc-84* alleles *n322* and *e1411*, which have missense mutations or small deletions in the amino terminus of UNC-84 (Fig. 7D) (Malone et al., 1999). We could not determine if UNC-83 protein was expressed at normal levels in *unc-84* class 1-3 mutants because our reagents do not function on Western blots. We conclude that UNC-84, and particularly the SUN domain of UNC-84, is required for UNC-83 localization to the envelope of migrating nuclei.

To determine if UNC-84 recruits UNC-83 to the nuclear envelope through a direct interaction, we performed GST pulldown assays. The SUN domain of UNC-84 fused to GST (UNC-84-SUN/GST) was attached to glutathione sepharose beads and used as the bait. As a negative control, GST alone was attached to beads and used as bait. [^{35}S]methionine-labeled UNC-83 bound to the UNC-84-SUN/GST-coated beads, but not the GST-coated beads (Fig. 7F). Addition of cold UNC-83/MBP competed with the [^{35}S]methionine-labeled UNC-83 so that only 39% of the [^{35}S]methionine-labeled UNC-83 was pulled down with the same amount of UNC-84-SUN/GST-coated beads (Fig. 7F). UNC-83 also interacts with itself in the same system (data not shown).

DISCUSSION

UNC-83 is a novel component of the nuclear envelope and is associated with migrating nuclei

Using a monoclonal antibody, we found that UNC-83 localized to the nuclear envelope of a number of different cell types. The nuclear envelope consists of an inner nuclear membrane connected through nuclear pores to an outer nuclear membrane, which is continuous with the endoplasmic reticulum (Gruenbaum et al., 2000). As UNC-83 colocalized with lamin and was not widely distributed throughout the endoplasmic reticulum, UNC-83 may be a component of the inner nuclear membrane. However, this hypothesis needs to be tested using electron microscopy.

UNC-83 first localized to the nuclear envelope of migrating hyp7 precursor nuclei. Later in development, UNC-83 was also detected in the endodermal cells. Both of these cell types have pronounced defects in nuclear migration in *unc-83* mutants, indicating a role for UNC-83 protein. However, UNC-83 was also detected at later stages of development in a wider variety of cell types, including several cells in the pharynx of comma-stage embryos and a number of hypodermal and other cells throughout the larval and adult stages. We do not know if UNC-83 functions in these cells.

The complex temporal pattern of UNC-83 expression may be controlled by enhancer elements spread throughout the large genomic region at the 5′ end of the gene. Each of the three *unc-83* transcripts has a 4-5 kb intron near its beginning (Fig. 2). Such introns are large compared with average *C. elegans* introns, and often contain complex regulatory regions and transcript-specific promoters (Blumenthal and Steward, 1997). Additionally, the large regulatory region may explain why we were unable to rescue the P cell nuclear migration phenotype. It is possible that the molecular lesions in the three *unc-83* alleles we failed to identify after determining the sequences of the entire predicted open reading frame reside within non-coding regulatory regions. Alternatively, these mutations may reside in the open reading frame of additional, unidentified *unc-83* transcripts. For example, the minimal rescuing fragment for the *unc-83* hyp7 nuclear migration phenotype does not contain a complete copy of any of the three identified transcripts and therefore may encode a distinct transcript.

We propose that the different *unc-83* transcripts are regulated in a tissue-specific manner. Specifically, we suggest that the shortest identified *unc-83* transcript, *unc-83C*, functions in hyp7 cells, while the longer ones, *unc-83A* and *unc-83B*, function in other tissues, including P cells and endodermal cells. Three observations support this model: (1) the *unc-83* molecular lesions that do not disrupt the nuclear migrations of hyp7 cells do not disrupt the shorter transcript (Fig. 4D); (2) RNAi directed against only the longer transcripts does not disrupt nuclear migration in the hyp7 cells, whereas RNAi directed against all three transcripts does disrupt hyp7 nuclear migration (Table 4); (3) we detected UNC-83 at the nuclear envelope of hyp7 cells in *unc-83(ku18)* embryos (Fig. 5), in which hyp7 nuclear migration is not disrupted, but not in P cells or endodermal cells, which are disrupted for nuclear migration.

UNC-83 is recruited to the nuclear envelope by UNC-84

The *unc-83* P-cell and hyp7 precursor nuclear migration defects we observed were similar to those previously described for null mutants of *unc-84* (Malone et al., 1999). In addition, the *unc-83* defect during intestinal nuclear migration was similar to the defects we observed in *unc-84(n369)* (a class 1, null allele) and *unc-84(e1410)* (a class 3 allele disrupting the conserved SUN domain; data not shown) mutants. However, *unc-84(e1174)* (a class 4 allele affecting the amino terminal end of UNC-84) only slightly disrupted intestinal nuclear migration (data not shown). In contrast to P-cell nuclear migration, intestinal nuclear migration events were cold sensitive, suggesting that a second partially redundant pathway can control intestinal nuclear migration.

As the phenotypes of *unc-83* and *unc-84* mutants are similar, we looked for a more direct interaction and found that mutations affecting the conserved SUN domain of UNC-84 disrupted the localization of UNC-83 (Fig. 7). This is different from *unc-83* mutations, which do not disrupt the localization of UNC-84::GFP (Malone et al., 1999). We therefore propose that the role of UNC-84 in nuclear migration is to recruit UNC-83 to the nuclear envelope. The cell specificity of UNC-83 localization to the nuclear envelope could be defined by the complex transcriptional regulation of *unc-83*. This role of UNC-84 could completely account for the nuclear migration defects observed in *unc-84* mutations. Consistent with this hypothesis, *unc-84; unc-83* double mutant animals have the same nuclear migration defect as animals with either mutation alone (Malone et al., 1999), and UNC-83 and UNC-84 colocalize at the nuclear envelope (see Fig. 6). It is likely that the SUN domain of UNC-84 recruits UNC-83 to the nuclear envelope by a direct physical interaction, as we showed that

the SUN domain of UNC-84 interacts with UNC-83 in vitro (Fig. 7F).

The role of UNC-83 in nuclear migration

What is the role of UNC-83 in nuclear migration? Defects in nuclear migration could potentially be caused by abnormalities in the association between centrosomes and nuclei, as centrosomes can be critical in nuclear migration (Raff and Glover, 1989; Reinsch and Gonczy, 1998). We previously proposed that UNC-84 and UNC-83 function in the nuclear membrane to attach centrosomes to the nucleus for nuclear migration (Malone et al., 1999). This model predicts that in an *unc-83* null mutant, centrosomes would migrate across the cell, but without functional UNC-83, the nucleus would fail to follow. Such a phenotype has been observed in both *C. elegans* early embryos and *Drosophila* embryos where mutations in the dynein heavy chain disrupt the centrosome to nuclear envelope association (Gonczy et al., 1999; Robinson et al., 1999). However, we found that in both hyp7 precursors and intestinal cells of *unc-83* mutant embryos, centrosomes remain associated with the nucleus despite a defect in nuclear migration (Fig. 2; Table 3). Therefore *unc-83* is not required for the attachment of centrosomes to nuclei.

Another possibility is that UNC-84 and UNC-83 interact with the nuclear matrix to maintain nuclear structure or promote dynein localization to the nuclear envelope during nuclear migration. These models predict that the nuclear matrix or dynein localization in *unc-83* and *unc-84* mutants would be disrupted. However, the nuclear matrix, at least as determined by lamin immunolocalization, appeared normal in *unc-83* mutant hyp7 cells (Fig. 3). We were unable to examine dynein in migrating nuclei, owing to high levels of cytoplasmic dynein. However it is unlikely that UNC-83 and UNC-84 are required for dynein localization to the nuclear envelope because knockout experiments with dynein cause early pronuclear migration defects not seen in *unc-83* or *unc-84* mutant embryos (Gonczy et al., 1999).

We propose a model inspired by a recent report about nuclear positioning in fission yeast. Tran et al. (Tran et al., 2001) propose that microtubules push the nucleus to the center of the cell by growing at their plus ends at the cell periphery. Interestingly they show that Sad1p, the *S. pombe* homolog of UNC-84, is concentrated at regions of the nuclear envelope in contact with microtubules as well as spindle pole bodies. This suggests a role for Sad1p, and a homologous role for UNC-84 and UNC-83, in the association of microtubules with the nuclear envelope. This model could explain the punctate appearance of UNC-83 on the nuclear envelope. We do note that tubulin staining, in at least embryonic intestinal cells, appears normal in *unc-83* or *unc-84* mutants, suggesting that *unc-83* nuclear migration defects are not caused by a gross disruption of microtubules. However, mutations in *unc-83* could be disrupting a localized association between microtubules and the nuclear envelope beyond the resolution of our assay. In this model, UNC-83 and UNC-84 would function as part of a bridge to transfer the forces required for nuclear migration through the nuclear envelope between the structural elements of the nucleus, including the lamina, to molecular motors of the cytoskeleton. Specifically, UNC-83 may function to connect microtubules to the nucleus independently of centrosomes.

We thank Gail Ackerman, Kurt Christensen and Erika Unzueta for raising the monoclonal antibody, which was generated with support from the NCI, University of Colorado Cancer Center Core Grant P30-CA46934. We thank Yossef Gruenbaum for the lamin antibody, Allan Coulson for cosmids, Yuji Kohara for ESTs, Scott Clark and Glen Herrmann for *unc-83* alleles, Leon Avery and the CGC for mapping strains, and members of the Han laboratory for advice. D. A. S. was supported by NIH postdoctoral grant F32-HL10449. G. H. was supported by a postdoctoral fellowship from the Damon Runyon-Walter Winchell Foundation (DRG1561). This research was supported by NIH grants GM47869 to M. H. and GM24663 to H. R. H., and The Howard Hughes Medical Institute, of which M. H., H. R. H. and J. R. P. are Investigators.

REFERENCES

Blumenthal, T. and Steward, K. (1997). RNA Processing and gene structure. In *C. elegans II* (ed. D. L. Riddle T. Blumenthal B. J. Meyer and J. R. Priess), pp. 117-146. Cold Spring Habor, NY: Cold Spring Harbor Laboratory Press.

Brenner, S. (1974). The genetics of *Caenorhabditis elegans. Genetics* **77**, 71-94.

Chytilova, E., Macas, J., Sliwinska, E., Rafelski, S. M., Lambert, G. M. and Galbraith, D. W. (2000). Nuclear dynamics in Arabidopsis thaliana. *Mol. Biol. Cell* **11**, 2733-2741.

Clark, S. G., Stern, M. J. and Horvitz, H. R. (1992). C. elegans cell-signalling gene sem-5 encodes a protein with SH2 and SH3 domains. *Nature* **356**, 340-344.

Davis, M. W., Fleischhauer, R., Dent, J. A., Joho, R. H. and Avery, L. (1999). A mutation in the C. elegans EXP-2 potassium channel that alters feeding behavior. *Science* **286**, 2501-2504.

Dobyns, W. B. and Truwit, C. L. (1995). Lissencephaly and other malformations of cortical development: 1995 update. *Neuropediatrics* **26**, 132-147.

Fan, S. S. and Ready, D. F. (1997). Glued participates in distinct microtubule-based activities in Drosophila eye development. *Development* **124**, 1497-1507.

Fire, A., Xu, S., Montgomery, M. K., Kostas, S. A., Driver, S. E. and Mello, C. C. (1998). Potent and specific genetic interference by double-stranded RNA in Caenorhabditis elegans. *Nature* **391**, 806-811.

Gonczy, P., Pichler, S., Kirkham, M. and Hyman, A. A. (1999). Cytoplasmic dynein is required for distinct aspects of MTOC positioning, including centrosome separation, in the one cell stage Caenorhabditis elegans embryo. *J. Cell Biol.* **147**, 135-150.

Gruenbaum, Y., Wilson, K. L., Harel, A., Goldberg, M. and Cohen, M. (2000). Review: nuclear lamins–structural proteins with fundamental functions. *J. Struct. Biol.* **129**, 313-323.

Hagan, I. and Yanmagida, M. (1995). The product of the spindle formation gene sad1+ associates with the fission yeast spindle pole body and is essential for viability. *J. Cell Biol.* **129**, 1033-1047.

Horvitz, H. R. and Sulston, J. E. (1980). Isolation and genetic characterization of cell-lineage mutants of the nematode Caenorhabditis elegans. *Genetics* **96**, 435-454.

Huang, X. Y. and Hirsh, D. (1989). A second trans-spliced RNA leader sequence in the nematode Caenorhabditis elegans. *Proc. Natl. Acad. Sci. USA* **86**, 8640-8644.

Kent, W. J. and Zahler, A. M. (2000). The intronerator: exploring introns and alternative splicing in Caenorhabditis elegans. *Nucleic Acids Res.* **28**, 91-93.

Kohara, Y. (1996). Large scale analysis of C. elegans cDNA. *Tanpakushitsu Kakusan Koso* **41**, 715-720.

Leung, B., Hermann, G. J. and Priess, J. R. (1999). Organogenesis of the Caenorhabditis elegans intestine. *Dev. Biol.* **216**, 114-134.

Liu, J., Ben-Shahar, T. R., Riemer, D., Treinin, M., Spann, P., Weber, K., Fire, A. and Gruenbaum, Y. (2000). Essential roles for caenorhabditis elegans lamin gene in nuclear organization, cell cycle progression, and spatial organization of nuclear pore complexes. *Mol. Biol. Cell* **11**, 3937-3947.

Malone, C. J., Fixsen, W. D., Horvitz, H. R. and Han, M. (1999). UNC-84 localizes to the nuclear envelope and is required for nuclear migration and anchoring during C. elegans development. *Development* **126**, 3171-3181.

McIntire, S. L., Reimer, R. J., Schuske, K., Edwards, R. H. and Jorgensen, E. M. (1997). Identification and characterization of the vesicular GABA transporter. *Nature* **389**, 870-876.

Melcher, K. and Johnston, S. A. (1995). GAL4 interacts with TATA-binding protein and coactivators. *Mol. Cell Biol.* **15**, 2839-2848.

Mello, C. C., Kramer, J. M., Stinchcomb, D. and Ambros, V. (1991). Efficient gene transfer in C.elegans: extrachromosomal maintenance and integration of transforming sequences. *EMBO J.* **10**, 3959-70.

Miller, D. M. and Shakes, D. C. (1995). Immunofluorescence microscopy. *Methods Cell Biol.* **48**, 365-394.

Morris, N. R. (2000). Nuclear migration. From fungi to the mammalian brain. *J. Cell Biol.* **148**, 1097-1101.

Mosley-Bishop, K. L., Li, Q., Patterson, L. and Fischer, J. A. (1999). Molecular analysis of the klarsicht gene and its role in nuclear migration within differentiating cells of the Drosophila eye. *Curr. Biol.* **9**, 1211-1220.

Okkema, P. G. and Fire, A. (1994). The Caenorhabditis elegans NK-2 class homeoprotein CEH-22 is involved in combinatorial activation of gene expression in pharyngeal muscle. *Development* **120**, 2175-2186.

Pruss, R. M., Mirsky, R., Raff, M. C., Thorpe, R., Dowding, A. J. and Anderton, B. H. (1981). All classes of intermediate filaments share a common antigenic determinant defined by a monoclonal antibody. *Cell* **27**, 419-428.

Raff, J. W. (1999). The missing (L) UNC? *Curr. Biol.* **9**, R708-R710.

Raff, J. W. and Glover, D. M. (1989). Centrosomes, and not nuclei, initiate pole cell formation in Drosophila embryos. *Cell* **57**, 611-619.

Raich, W. B., Agbunag, C. and Hardin, J. (1999). Rapid epithelial-sheet sealing in the Caenorhabditis elegans embryo requires cadherin-dependent filopodial priming. *Curr. Biol.* **9**, 1139-1146.

Reiner, O., Carrozzo, R., Shen, Y., Wehnert, M., Faustinella, F., Dobyns, W. B., Caskey, C. T. and Ledbetter, D. H. (1993). Isolation of a Miller-Dieker lissencephaly gene containing G protein beta-subunit-like repeats. *Nature* **364**, 717-721.

Reinsch, S. and Gonczy, P. (1998). Mechanisms of nuclear positioning. *J. Cell Sci.* **111**, 2283-2295.

Robinson, J. T., Wojcik, E. J., Sanders, M. A., McGrail, M. and Hays, T. S. (1999). Cytoplasmic dynein is required for the nuclear attachment and migration of centrosomes during mitosis in Drosophila. *J. Cell Biol.* **146**, 597-608.

Sulston, J. E. and Horvitz, H. R. (1977). Post-embryonic cell lineages of the nematode, Caenorhabditis elegans. *Dev. Biol.* **56**, 110-156.

Sulston, J. E. and Horvitz, H. R. (1981). Abnormal cell lineages in mutants of the nematode Caenorhabditis elegans. *Dev. Biol.* **82**, 41-55.

Sulston, J. E., Schierenberg, E., White, J. G. and Thomson, J. N. (1983). The embryonic cell lineage of the nematode *Caenorhabditis elegans*. *Dev. Biol.* **100**, 64-119.

Sundaram, M. and Han, M. (1995). The C. elegans ksr-1 gene encodes a novel Raf-related kinase involved in Ras-mediated signal transduction. *Cell* **83**, 889-901.

Tomlinson, A. (1985). The cellular dynamics of pattern formation in the eye of Drosophila. *J. Embryol. Exp. Morphol.* **89**, 313-331.

Tran, P. T., Marsh, L., Doye, V., Inoue, S. and Chang, F. (2001). A mechanism for nuclear positioning in fission yeast based on microtubule pushing. *J. Cell Biol.* **153**, 397-411.

Trent, C., Tsung, N. and Horvitz, H. R. (1983). Egg-laying deffective mutants of the nematode *Caenorhabditis elegans*. *Genetics* **104**, 619-647.

Wu, Y. and Han, M. (1994). Suppression of activated Let-60 ras protein defines a role of Caenorhabditis elegans Sur-1 MAP kinase in vulval differentiation. *Genes Dev.* **8**, 147-159.

Yochem, J., Gu, T. and Han, M. (1998). A new marker for mosaic analysis in Caenorhabditis elegans indicates a fusion between hyp6 and hyp7, two major components of the hypodermis. *Genetics* **149**, 1323-1334.